On Representation of Lightning Return Stroke as a Lossy Monopole Antenna With Inductive Loading

Siamak Bonyadi-Ram, Rouzbeh Moini, *Senior Member, IEEE*, S. H. H. Sadeghi, *Senior Member, IEEE*, and Vladimir A. Rakov, *Fellow, IEEE*

***Abstract*—In this paper, a modification of the antenna theory (AT) model of the lightning return stroke to include inductive loading is presented. The distributed inductive energy-storing elements are used in the modified AT model (designated as ATIL model, where IL stands for inductive loading) to control the propagation speed of the upward traveling current wave without using an artificial, higher permittivity dielectric medium, as done in the original AT model. The variation of the propagation speed along the channel is also considered in the proposed model. As in the original AT model, resistive loading is used to account for the current attenuation with height. Numerical solution of the electric field integral equation in the time domain using the method of moments with appropriate boundary conditions yields a time–space distribution of current along the lightning channel. This current distribution and the resultant electromagnetic fields for the ATIL model are compared with those predicted by other time-domain and frequency-domain electromagnetic models. The current distribution predicted by the ATIL model exhibits features (such as current dispersion) that are more consistent with optical observations of lightning compared to the predictions of the original AT model.**

***Index Terms*—Antenna theory (AT), current distribution, electric and magnetic fields, inductive loading, lightning return stroke modeling.**

I. Introduction

MODELING of the lightning return stroke typically involves a description of the time and height variations of the current wave along the channel, which is needed for calculation of resultant electromagnetic fields. Reviews and comparisons of the most common models can be found in [1]–[5]. The so-called engineering models, such as the transmission line (TL), modified transmission line exponential (MTLE), modified transmission line linear (MTLL), traveling current source (TCS), and Diendorfer–Uman (DU) models relate current distribution at a given height along the lightning channel to the current at the channel base [4]. Outputs of an adequate model should be consistent with the observed characteristics of the return stroke such as the variation of light intensity with height (which probably reflects variations in the intensity of the current wave along the channel), propagation speed of the luminosity front (often used as a proxy for the current wave front), and electromagnetic fields at different distances from the channel.

Most of the commonly used models assume a constant current propagation speed, although it is known that the return-stroke speed varies with height along the lightning channel [6]. For example, Idone and Orville [7] observed a decrease of the optical wave front propagation speed with height for both first and subsequent strokes. Borovski [8] presented an electromagnetic model of the return stroke (and leader) in which the wave propagation speed is a function of physical characteristics (radius and temperature) of the channel and also of the risetime of the current waveform at the channel base. Baum [9] and Baum and Baker [10] developed a distributed circuit model in which the return-stroke speed is determined by dynamics of channel corona sheath. Wang *et al.* [11], using a high-speed digital optical measurement system, examined the propagation characteristics of leaders and return strokes in the triggered lightning from experiments conducted at Camp Blanding, Florida. Their resultant return-stroke speed profiles within 400 m height above ground showed dependency of the speed on height, although it might be due, at least in part, to different propagation conditions along the metal-vapor-contaminated and natural channel sections. Some of the models, such as the modified DU (MDU) [3], variable discharge time constant (VDTC) [2], and the model of Podgorski and Landt [12], considered variation of the propagation speed with height. Further discussion of the return-stroke speed as a function of height is found in a recent review by Rakov [6].

Studying the propagation speed is also important from the point of view of comparing radiated electromagnetic fields predicted by models with field measurements. The effect of return-stroke speed on the radiated electromagnetic field waveforms has been studied by Rakov and Dulzon [13] and Rubinstein and Uman [14]. Tottappillil and Uman [2] showed that taking into account the variable propagation speed resulted in a better overall agreement of calculated and measured electric field waveforms.

The antenna theory (AT) model [15], [16] belongs to the category of electromagnetic models, and represents the lightning channel as a lossy monopole antenna above a perfectly conducting ground. The spatial and temporal distribution of current along the antenna was determined by solving the electric field integral equation (EFIE) using the method of moments (MoMs) in the time domain [15]–[18]. A constant, lower than the speed of light propagation speed was achieved by setting the relative

Manuscript received July 11, 2006; revised January 22, 2007 and June 2, 2007. This work was supported by Iran Telecommunication Research Center.

S. Bonyadi-Ram is with the Electromagnetics Research Laboratory, Amirkabir University of Technology, Tehran 15914, Iran (e-mail: bonyadi@cra.ir).

R. Moini and S. H. H. Sadeghi are with the Electromagnetics Research Laboratory, Amirkabir University of Technology, Tehran 15914, Iran (e-mail: moini@aut.ac.ir; sadeghi@aut.ac.ir).

V. A. Rakov is with the Electrical and Computer Engineering Department, University of Florida, Gainesville, FL 32611 USA (e-mail: rakov@ece.ufl.edu).

Digital Object Identifier 10.1109/TEMC.2007.913221

permittivity ε_r of the surrounding medium to a value greater than that of free space. In order to set the propagation speed at 1.3×10^8 m/s in this model, one should use ε_r equal to 5.3. An increase of ε_r serves to increase the capacitance of the channel, while the inductance remains constant, and therefore, simulates the radial corona sheath surrounding the lightning channel core [16]. It is important to note that the assumption of $\varepsilon_r > 1$ was only used to find the current distribution along the channel, which was then allowed to radiate into free space with $\varepsilon_r = 1$ [17]. However, even the current distribution along the channel can be potentially influenced to some (presumably small) extent by the unrealistic assumption $\varepsilon_r > 1$.

In the model presented in this paper, in order to control the return-stroke speed, inductive energy-storing elements are included in the antenna representation of the lightning channel. The use of energy-storing elements in the antenna and TL studies has been previously described in a number of works. The induction phenomenon in solving electrical circuits using the time-domain EFIE was studied by Bost *et al*. [19]. Guedira [20] applied local inductive and capacitive loads to the feeding point of a dipole antenna and determined resultant antenna currents. The additional distributed capacitance has been used to describe the effect of corona on TLs [21]. Applying shunt distributed capacitive loads, representing the radial corona sheath, to an antenna introduces some difficulties, as discussed by Bonyadi-Ram *et al*. [22]. One difficulty is related to the fact that distributed shunt capacitors require a return conductor parallel to the antenna, which turns the monopole antenna to an TL. Since the phase velocity is a function of the product of the inductance and capacitance (each per unit length), appropriately selected series distributed inductance can be used, instead of distributed shunt capacitance, to simulate the corona effect on the propagation speed [23]. Such an approach was previously used by Baba and Ishii [24] in their frequency-domain electromagnetic model.

In this paper, a modification is made in the original AT model [16] to include inductive loading of the channel in order to avoid the unrealistic assumption of higher permittivity of the surrounding medium. The variation in the propagation speed of the upward traveling current wave along the channel is also considered. Current distributions along the channel and the associated radiated electromagnetic fields for the new model are discussed and compared with those predicted by other time-domain and frequency-domain electromagnetic models. Besides the more realistic speed profile, dispersion of the channel current is better reproduced in the new model. The proposed model is a step forward to finding a method to reduce the speed of current waves propagating on a vertical conductor in air, such that the evolution of wave shape is consistent with optical observations of lightning.

II. Theory

The general electromagnetic formulation used in this paper is similar to that given in [16] and [17]. In the AT model with inductive loading (ATIL model), a set of distributed inductive loads is additionally applied to the simulated lightning channel. For resistive–inductive loading, the voltage on the loaded element $v(\mathbf{s}_L, t)$, can be related to the current on it, $i(\mathbf{s}_L, t)$, using the relation

$$v(\mathbf{s}_L, t) = Ri(\mathbf{s}_L, t) + L(\mathbf{s}_L)\frac{\partial i(\mathbf{s}_L, t)}{\partial t} \tag{1}$$

where $L(\mathbf{s}_L)$ and R are the height-dependent inductance and height-independent resistance located in the element denoted by s_L. Lightning channel and its image were discretized, appropriate boundary condition on the tangential electric field component was applied to each segment, and the resultant matrix-form equation is numerically solved according to the method introduced by Miller [25] and previously used in [16]. In order to avoid numerical instabilities, time Δt and space ΔR, discretization intervals are selected so that $c\Delta t \leq \Delta R$, where c is the speed of light [25]. The solution of this equation is presented in the form of a spatial-temporal current distribution along the antenna. It should be noted that the formulation used in [16] and [18] and also the modification employed here are general in that there is no limitation on the shape of the channel. Here, in order to facilitate comparison with the simulation results obtained using the original AT model, only a straight vertical channel above a perfectly conducting ground is considered.

III. Relation Between Speed and Inductive Loading in the ATIL Model

An unloaded horizontal, perfectly conducting wire above perfectly conducting ground behaves as a lossless uniform TL, and propagation speed along the wire is constant and equal to the speed of light$c = 1/\sqrt{L_0 C_0}$, where L_0 and C_0 are per unit length inductance and capacitance, respectively. Strictly speaking, this speed is not applicable to a vertical monopole antenna, and its image because the per unit length capacitance and inductance of such an antenna vary with height. As a result, the equivalent TL is nonuniform and the propagation speed is slightly lower than the speed of light. Further, in the case of lightning, the speed is reduced (typically by a factor of two or three) relative to the speed of light due to the presence of corona sheath and transformation of the leader channel to the return-stroke channel. Also, as noted above, the optically observed speed decreases with increasing height (we do not consider here the nonmonotonic variation of speed with height reported by Olsen *et al*. [26]). The bottom line here is that considering the lightning channel as a vertical wire above ground with its intrinsic capacitance and inductance per unit length does not allow one to reproduce observed lightning return-stroke speed profiles.

If we introduce an additional, height-variable distributed inductance along the antenna without any resistive loading, the resultant height-variable propagation speed along the simulated lightning channel will be given by

$$v(z) = \frac{1}{\sqrt{L'(z)C_0(z)}} = \frac{1}{\sqrt{(L_0(z) + L^{\mathrm{add}}(z))C_0(z)}} \tag{2}$$

where $L^{\mathrm{add}}(z)$ is the additional height-dependent distributed inductance per unit length. As a result, for a specified

height-variable speed $v(z)$, $L^{\mathrm{add}}(z)$ is given by

$$L^{\mathrm{add}}(z) = \frac{1}{\upsilon^2(z)C_0(z)} - L_0(z). \tag{3}$$

The capacitance C_0 (in farads per meter) and inductance L_0 (in henrys per meter) per unit length for a cylindrical metallic wire of radius a can be estimated using the following equations given by Bazelyan *et al*. [27] and Kodali *et al*. [28] (see also [33])

$$C_0(z) = \frac{2\pi\varepsilon_0}{\ln(2z/a)} \tag{4}$$

$$L_0(z) = \frac{\mu_0}{2\pi}\ln(2z/a) \tag{5}$$

where z is the height above ground. Applicability of these equations, derived for a horizontal wire above ground, to a vertical conductor is discussed by Kodali *et al*. [28]. Considering typical speed profiles for lightning shows that the values of intrinsic capacitance and inductance of an ideal cylindrical antenna above a perfectly conducting ground given by (4) and (5) cannot yield the variation of speed as specified by (2), and hence, an additional height-variable reactive element is needed to simulate such a speed profile. Note that additional distributed inductance along the channel has no physical meaning and is invoked only to reduce the speed of current wave to a value lower than the speed of light.

In the following, we will consider two types of inductive loading: fixed (uniform) and height varying (nonuniform). In the ATIL model with fixed inductive loading (ATIL-F), additional inductance per unit length was selected (by trial and error) so that to obtain a specified average speed. It turned out that fixed loading results in an almost uniform speed profile, as discussed in Section IV-B3 given later. For example, $L^{\mathrm{add}} = 8.0 \times 10^{-6}$ H/m results in $\upsilon = 1.3 \times 10^8$ m/s. Interestingly, this value of L^{add} is approximately equal to L^{add} that is computed from (3) using constant values C_0 and L_0 evaluated at $a = 0.02$ m and $z = 3500$ m from (4) and (5), respectively. Note that the values of C_0 and L_0 at $z = 3500$ m are applied to the entire channel. This is a commonly used simplification [28] based on the fact that the dependencies of C_0 and L_0 on z are weak (logarithmic). In the ATIL model with variable inductive loading (ATIL-V), a speed profile was chosen to achieve acceptable consistency with the published optical measurements. Optical observations are mainly limited to the visible part of the channel, usually extending from ground to a height of 1–3 km. The return-stroke speed typically decreases by 25% or more over the visible part of the channel with respect to the speed at the bottom of the channel [7]. In this paper, we use an exponentially decaying speed profile $\upsilon(z)$ that is described by the equation

$$\upsilon(z) = \upsilon_h - (\upsilon_h - \upsilon_0)\, e^{-\frac{z}{\lambda}} \tag{6}$$

where λ is the decay height constant, υ_0 is the propagation speed at the channel base (at ground level), and the final speed at the upper end of the channel (at $z = h$) asymptotically approaches υ_h. Tottappillil and Uman [2] have used a similar relation in the MDU model in which $\upsilon_h = 0$, i.e., the speed tends to zero at larger altitudes. The use of a nonzero value of υ_h gives us more control of the propagation speed profile, especially in the upper part of the channel. Optical observations have shown that the propagation speed near the bottom of the channel varies between $c/2$ and $c/3$ [9] and decreases with height. In this paper, we computed a speed profile along a 3.5 km lightning return-stroke channel using (6) with $\lambda = 450$ m, $\upsilon_0 = 1.6 \times 10^8$ m/s, and $\upsilon_h = 0.9 \times 10^8$ m/s. This profile is shown in Fig. 1. Note that, at $z = 3.5$ km, $\upsilon = 0.9 \times 10^8$ m/s, which is essentially equal to the assumed value of υ_h. It should be noted that there is essentially no limitation on the length of analyzed channel. Longer lightning channels could be analyzed if the information on speed profile were available.

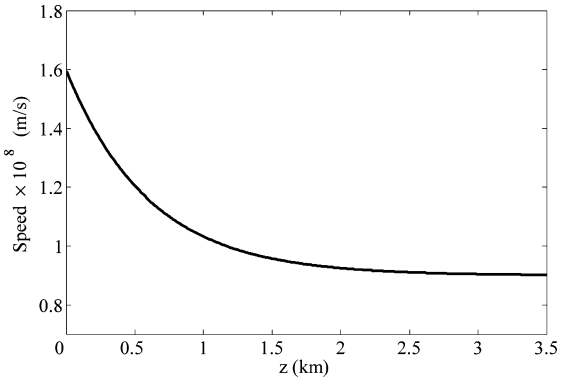

Fig. 1. Propagation speed as a function of height for the ATIL-V model obtained using (6) with $\lambda = 450$ m, $\upsilon_0 = 1.6 \times 10^8$ m/s, and $\upsilon_h = 0.9 \times 10^8$ m/s.

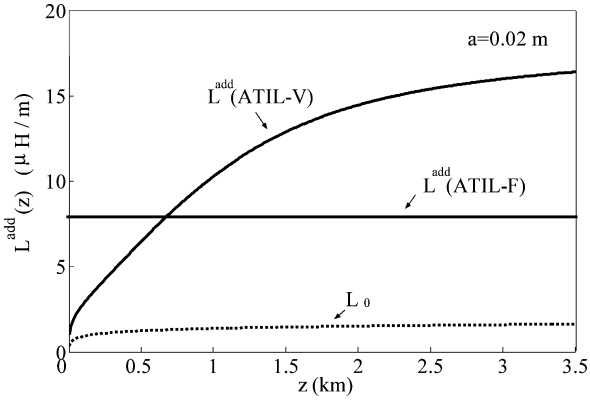

Fig. 2. Additional distributed inductance per unit length L^{add}, as a function of height for the ATIL-V [computed using (3)] and ATIL-F (determined by trial and error) models. The speed profile for the ATIL-V model is shown in Fig. 1, and the speed for the ATIL-F is 1.3×10^8 m/s. Also shown is the intrinsic inductance of the monopole antenna computed using (5) L_0, as a function of height.

In time-domain methods, the length of analyzed channel is limited by duration of analysis. We selected the analysis duration such that the traveling wave will never hit the top of the channel. This is a widely used approach in lightning research [4].

The corresponding additional distributed inductance as a function of height, calculated using (3), is depicted in Fig. 2. The $L_0(z)$ and $L^{\mathrm{add}}(z)$ profiles for the ATIL-F model with $\upsilon = 1.3 \times 10^8$ m/s are also shown in Fig. 2 for comparison.

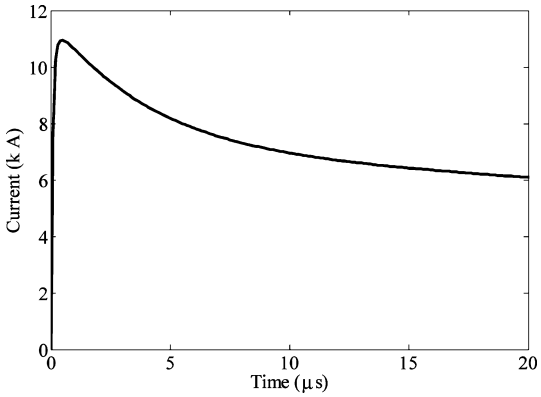

Fig. 3. Channel base current waveform used for the comparison of the AT [16] and ATIL models.

IV. Comparison of the ATIL Model With Previous Electromagnetic Models

A. Frequency-Domain Model of Baba and Ishii [24]

In this section, we compare predictions of the ATIL-F model with those of the model proposed by Baba and Ishii [24], who applied a set of uniform distributed inductive and resistive loads to the wire representing the lightning channel. The loaded channel was then used in a frequency-domain electromagnetic model employing a numerical electromagnetic code (NEC-2). The resultant current distribution along the channel and associated electric fields were presented. The uniform inductive loading in the model of Baba and Ishii resulted in an essentially constant propagation speed along the channel. This is why we compared their results with prediction of the ATIL-F (essentially constant speed) model. We considered both the current profiles and radiated electric fields, although detailed results (computed waveforms) are not presented here. The current distributions predicted by the two models (for the same channel geometry and excitation) are in fairly good agreement in terms of main features of current waveforms. Electric field waveforms at 5 and 100 km for the two models were in fairly good agreement, but appreciable differences (although within the range of variation of measured waveforms) were seen in the model-predicted electric fields at 50 m. The ATIL-V model can be viewed as a generalization of Baba and Ishii's model to reproduce any return-stroke speed profile.

B. Time-Domain Model of Moini et al. [16]

In this section, we compare the ATIL-F and ATIL-V models with the AT model presented by Moini *et al.* [16]. We consider a lightning channel with a height of 3.5 km and radius of 0.02 m above a perfectly conducting ground. The current at the channel base is the same as that used in [16] and shown in Fig. 3. The inductance per unit length for the ATIL-F model is set to $L^{\mathrm{add}} = 8.0 \times 10^{-6}$ H/m. Distributed resistance of the channel for the ATIL-F model is 0.5 Ω/m, considerably larger than 0.07 Ω/m in the AT model. For the AT model, ε_r is set to 5.3, while for both versions of the ATIL model, $\varepsilon_r = 1$. For the ATIL-V model, we used the profile of the distributed inductance shown in Fig. 2, and distributed resistance was set to 0.45 Ω/m. The reason for using different values of distributed resistance in the AT (0.07 Ω/m), ATIL-F (0.5 Ω/m), and ATIL-V (0.45 Ω/m) models will be discussed in the next section. The length of each channel segment was 10 m for all three models.

1) Current Profiles: Fig. 4(a)–(c) illustrates the current distribution along the channel for the AT, ATIL-F, and ATIL-V models. There are appreciable differences between the AT and ATIL-F models in terms of the general shape of current waveforms. The effect of height-variable speed can also be observed in the current distribution for the ATIL-V model. Both versions of the ATIL model predict more pronounced current dispersion (will be further discussed in Section IV-B2) than the AT model. The current dispersion (an increase in current pulse risetime with height) can also be observed in the current distribution predicted by the model of Baba and Ishii [24]. Different values of distributed resistance have been used in the published time-domain and frequency-domain models [4]. In this paper, in order to facilitate comparison with AT-model results, we assumed the same attenuation rate for all models, which required larger distributed resistances in the ATIL models, compared to the AT model. This additional distributed resistance in the ATIL models can be described using the TL theory. The square of attenuation factor for a TL is given by the formula

$$\alpha^2 = \mathrm{Re}\left[(R + j\omega L)\,(G + j\omega C)\right] \tag{7}$$

where R, L, G, and C are per unit length resistance, inductance, conductance, and capacitance of the TL, respectively, ω is the angular frequency, $j = \sqrt{-1}$, and "Re" stands for the real part of a complex quantity. This equation can be rewritten in the form

$$\alpha^2 = \mathrm{Re}\left[(RG + jRC\omega + jLG\omega - LC\omega^2)\right] = RG - LC\omega^2 \tag{8}$$

or

$$\alpha = \sqrt{RG - LC\omega^2}. \tag{9}$$

Equation (9) shows that the attenuation factor decreases with increasing L, and hence, in order to have a constant α, R should be increased.

In the AT model, the current attenuation in the lower sections of the channel is more pronounced than for both versions of the ATIL model. In other words, the attenuation is reduced in the presence of inductive loads, although the distributed resistance for both versions of the ATIL model is greater than that for the AT model. As can be seen in Fig. 2, the ATIL-V model employs smaller values of inductance in the lower sections of the channel than the ATIL-F model does, and hence, more attenuation is observed for the ATIL-V model. Both versions of the ATIL model predict more or less similar attenuation in the higher sections of the channel due to similar amounts of inductive and resistive loading.

2) Current Dispersion: It is clear that the ATIL-F and ATIL-V models [see Fig. 4(b) and (c)] predict considerably

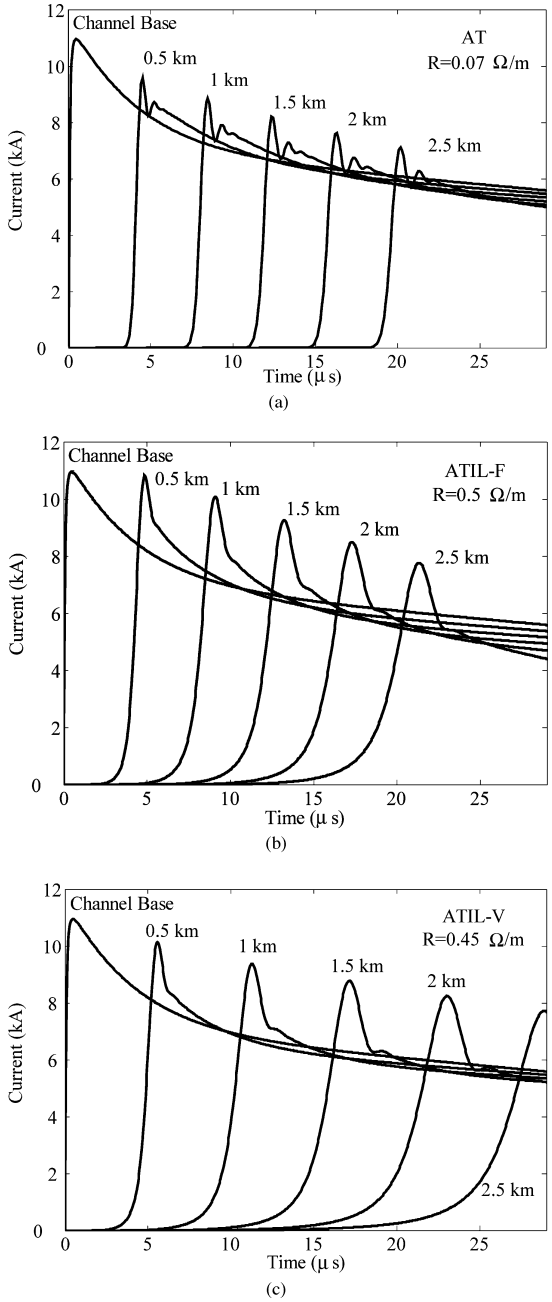

Fig. 4. Current distributions along the channel. (a) AT model. (b) ATIL-F model. (c) ATIL-V model. Shown are current versus time waveforms at the channel base and at heights of 500 m, 1 km, 1.5 km, 2 km, and 2.5 km above ground.

larger current dispersion than the AT model does [see Fig. 4(a)]. This larger dispersion is in agreement with optical observations of Jordan and Uman [29] and Wang *et al.* [11]. The observed current dispersion in the inductively loaded channel can be explained using the TL theory. The upward traveling current wave in the channel can be decomposed into two components [30].

1) Antenna-mode current, which is governed by the scattering theory. The propagation speed of this component is equal to the electromagnetic wave propagation speed v, in the surrounding medium, which is the speed of light when $\varepsilon_r = 1$.
2) TL-mode current, which is governed by the TL theory and propagates at an adjusted speed $v(z)$.

The propagation speed of each of the two current components is a function of ε_r. The AT model yields a full wave solution for the current distribution along the metallic structure including both the TL-mode and antenna-mode currents [4]. The resultant current-wave propagation speed is a function of relative permittivity of the medium. Adding distributed inductive loads as the circuit elements to the discretized EFIE dramatically affects the propagation speed of the TL-mode current because the current passes through loaded segments. On the other hand, the antenna-mode component of the current is independent of the circuit elements because loaded segments do not play dominant role in the electromagnetic coupling between the segments. Different propagation speeds for the two current components result in noticeable current dispersion along the channel, which increases with height. Additional discussion of current dispersion is found in Appendix A.

3) Speed Profile: In this section, the variation of return-stroke speed along the channel predicted by the AT, ATIL-F, and ATIL-V models is presented. The choice of tracking point will affect the model-predicted speed, since the shape of current (or luminosity) waveform changes with height. Olsen *et al.* [26] obtained different speed values tracking different reference points, including 10%, 20%, 90%, and 100% of peak, as well as the maximum rate of rise of the return-stroke luminosity pulse. The point of initial deflection from zero level is usually masked by noise, and hence, difficult to identify in optical measurements. We have chosen 10%, 20%, and 100% of peak, and the maximum time derivative of current waveform (the latter corresponds to the time at witch the current waveform reaches its maximum rate of rise, di/dt) as reference points. Speed v_k in segment k is calculated at the center of the segment by dividing the vertical distance between adjacent viewed heights $h_k - h_{k-1}$, by the tracked time interval $t_k - t_{k-1}$. The resultant speed profiles for the AT, ATIL-F, and ATIL-V models are shown in Fig. 5(a)–(c). In order to facilitate direct comparison, the "theoretical" speed profiles [given by (6) for the ATIL-V model or constant value equal to 1.3×10^8 m/s for the AT and ATIL-F models] are also shown in this figure. The current peak and di/dt peak speed profiles at heights greater than some hundreds of meters above ground are fairly similar to the theoretical profiles for the AT and the ATIL-V models. The estimated speed at lower sections of the channel is noticeably greater than the theoretical speed. This may be due to significant changes in current wave shape in the lower sections of the channel [for example, compare current wave shapes at the channel base and at a height of 500 m above ground in Fig. 4(a)]. Propagation speeds for the AT and ATIL-F, as expected, are almost constant over the entire channel length considered. The difference between speeds obtained from the four estimated profiles (current peak, peak of di/dt, 10%, and 20% of the peak) for the AT model is less than those predicted by the ATIL-F and the ATIL-V models. This is because of lower current dispersion predicted by the AT model. It can also be observed that tracking a lower percentage of peak results in a higher propagation speed, which is in agreement with optical data reported in [26]. It is also observed

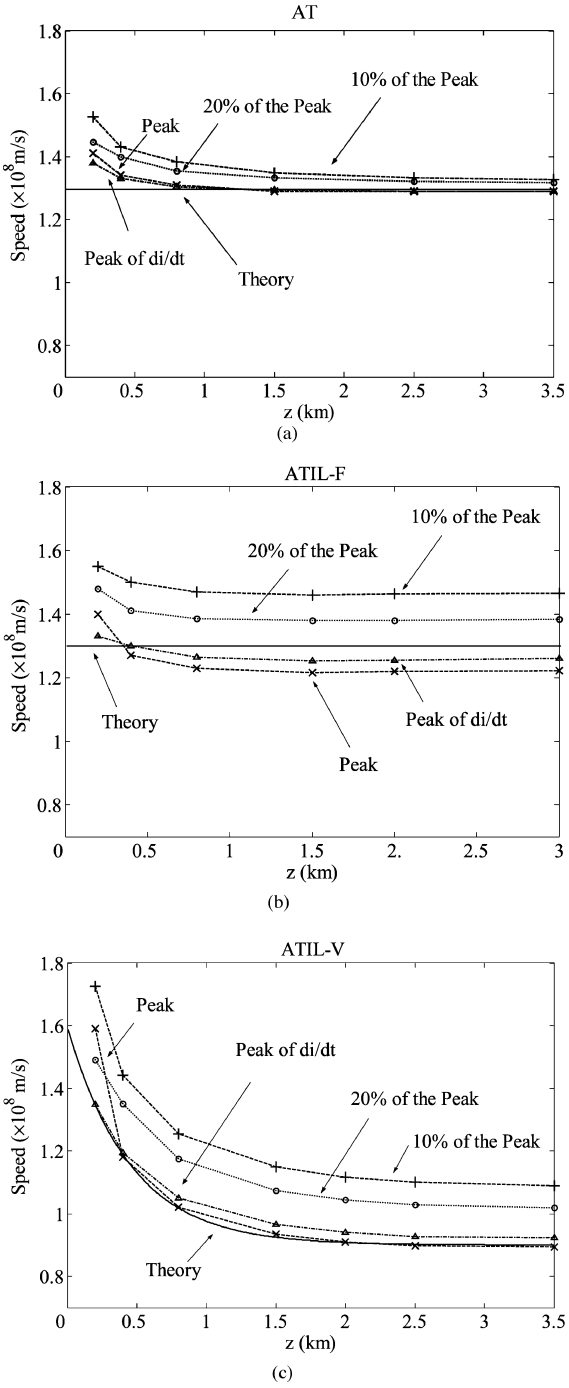

Fig. 5. Return-stroke speed profiles for (a) the AT, (b) ATIL-F, and (c) ATIL-V models obtained using different reference points on the current waveform, peak, 10% of peak, 20% of peak on the wave front, and peak of d*i*/d*t*. "Theoretical" speed profiles, $v = 1.3 \times 10^8$ m/s = constant, for the AT and ATIL-F models and the curve shown in Fig. 1 for the ATIL-V, are also shown.

that both versions of the ATIL model predict propagation speeds that appear to be nearly equal to the speed of light if the point of initial deflection from zero level is tracked, while in the AT model, the propagation speed remains near 1.3×10^8 m/s. This difference is expected, since in both versions of the ATIL model, the antenna-mode current propagates at the speed of light, while in the AT model, it propagates at $v = 1.3 \times 10^8$ m/s (see Appendix A).

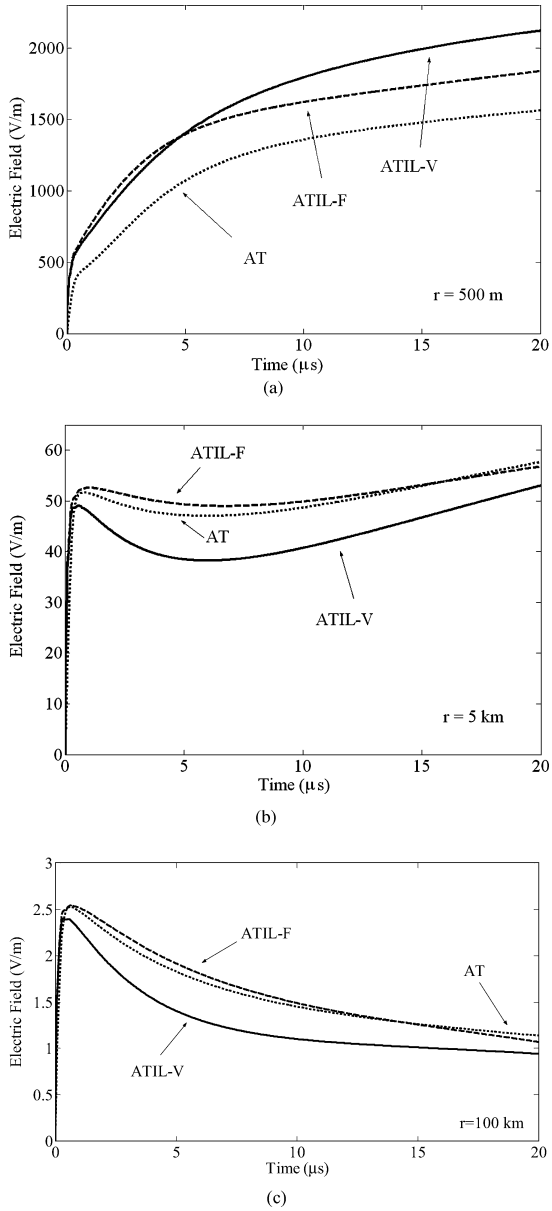

Fig. 6. Vertical component of electric field for the AT, ATIL-F and ATIL-V models calculated (a) $r = 500$ m, (b) $r = 5$ km, and (c) $r = 100$ km from the lightning channel whose parameters are given in Section IV-B.

4) Electromagnetic Fields: Fig. 6(a)–(c) and Fig. 7(a)–(c) illustrate the electric and magnetic fields, respectively, at three different distances, 500 m, 5 km, and 100 km from the lightning channel base calculated using the AT, ATIL-F, and ATIL-V models. The fields are computed using the equations employed in [16] (see, for example, [4, eqs. (6) and (7)]).

At $r = 500$ m, after 10 μs, all three examined models predict similar magnetic field waveforms. The ATIL-F model predicts a higher initial peak of the magnetic field than the other two models, since the current in the lower parts of the channel for the ATIL-F is greater than for the other two models (see Fig. 4). On the other hand, the time of the magnetic field peak for the AT model is greater than those for the AILT-F and ATIL-V models. At $r = 500$ m, predicted electric fields prior

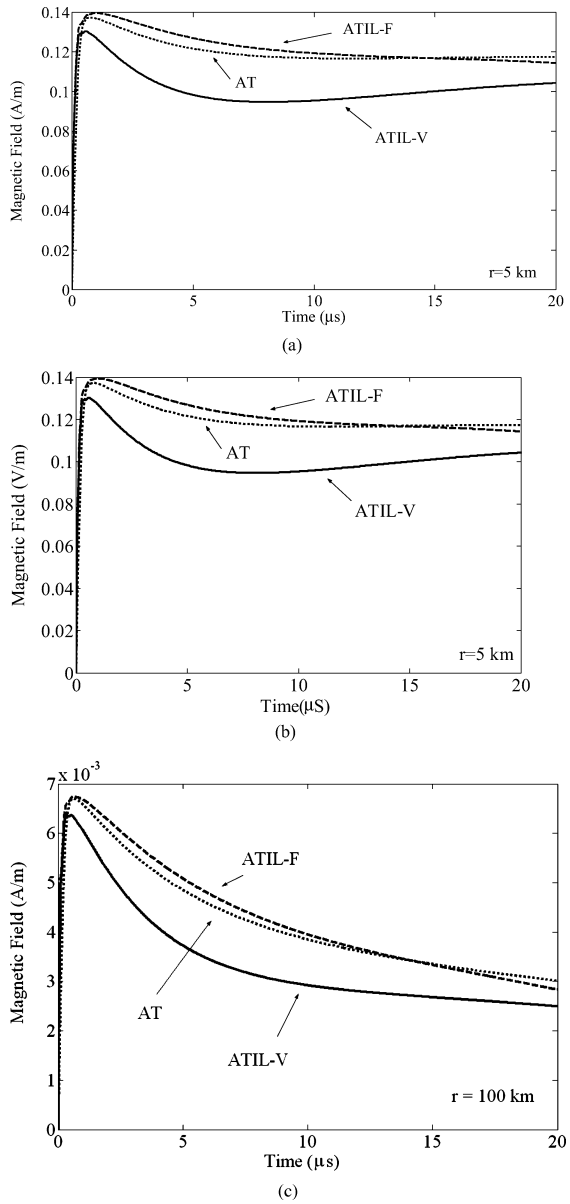

Fig. 7. Horizontal component of magnetic field calculated at different distances from the lightning channel with the parameters defined in Section IV-B for the AT, ATIL-F, and ATIL-V models. (a) $r = 500$ m. (b) $r = 5$ km. (c) $r = 100$ km.

to 1 μs for both ATIL-F and ATIL-V models are nearly identical, which suggests that the variation of propagation speed cannot alter the electric field waveform at close distances during the first microsecond or so. The AT model predicts the lowest electric field, while its rising slope after 5 μs is similar to that for the ATIL-F model. Due to higher propagation speed in the lower part of the channel for the ATIL-F model, after 1 μs, this model predicts the steepest electric field slope as well as a greater final field value. The AT model and both versions of the ATIL model do not show the magnetic field hump at 50 μs that can be seen in typical measured waveforms of [31].

The electric and magnetic fields at 5 km are more or less similar for all the models considered. The ATIL-V model predicts a smaller overall electric or magnetic field value, a steeper falling slope after the initial peak, and a higher rising slope than the other two models, which is more consistent with the typical waveforms measured at 5 km [31]. This is because of a higher propagation speed in the lower sections of the lightning channel (causes a steeper falling slope) and a lower speed in higher parts of the channel (results in a higher rising slope) in the ATIL-V model.

At 100 km, the electric and magnetic field wave shapes are similar. At this distance, the ATIL-V predicts lower fields than the other two models. This is due to a lower propagation speed in the upper part of the lightning channel that causes a greater delay in illuminating higher parts of the channel [compare the current at 2500 m at 20 μs in Fig. 4(a)–(c)]. During the initial 13 μs or so, the ATIL-F and the AT models exhibit fairly similar behavior in predicting far electromagnetic fields, while the ATIL-V model predicts a lower peak and a steeper falling slope after the peak. Due to a lower propagation speed in the upper part of the channel, the final falling slope for the ATIL-V is less than that for the other two models considered. None of the three models considered here can predict zero crossing within about 50–60 μs, as typically seen in most waveforms measured at this distance.

V. Summary

In this paper, a modification of the AT model of the lightning return stroke is introduced. In the proposed model, the lightning channel is represented by a lossy vertical monopole antenna above a perfectly conducting ground loaded by a set of constant (ATIL-F) or height-variable (ATIL-V) distributed inductances, fed at its lower end by a voltage source. The spatial and temporal distribution of the current along the channel is obtained by solving EFIE with the suitable boundary conditions, using the MoMs in the time domain. The ATIL-V model allows one to have more control of the variation of propagation speed along the channel and also of the current distribution and resultant electromagnetic field waveforms without artificially changing the relative permittivity of the surrounding medium, as done in the original AT model. The ATIL-F and ATIL-V models are compared to other frequency-domain and time-domain electromagnetic models in terms of the current distribution along the channel and remote electromagnetic fields. The current dispersion predicted by both the ATIL-F and ATIL-V models is more consistent (relative to the original AT model) with optical observations of lightning. It is shown that the adjusting relative permittivity of the surrounding medium, as done in the AT model, does not affect current dispersion along the channel, while in both versions of the ATIL model, the current dispersion increases with increasing propagation speed. The validity of lightning return-stroke models is most conveniently tested by comparing model-predicted remote fields with typically measured ones. Our subjective assessment of agreement of salient features of the models considered in this paper and model-predicted fields with optical observations of lightning (speed profile and light pulse dispersion which is used as a proxy for current pulse dispersion) and typical field measurements [31], respectively, is presented in Table I. Since

TABLE I
CONSISTENCY OF MODEL PREDICTIONS WITH MEASUREMENTS

Characteristics / Models	Current-wave propagation speed profile	Current dispersion	Remote electric fields	Remote magnetic fields
Model of Baba and Ishii [24]	Moderate	Good	Moderate	Moderate
AT model (Moini *et al.* [16])	Moderate	Moderate	Moderate	Moderate
ATIL-F (this study)	Moderate	Good	Moderate	Moderate
ATIL-V (this study)	Good	Good	Moderate	Moderate

the concept of inductive loading in the frequency-domain model of Baba and Ishii [24] and in the ATIL-F model is essentially the same, predictions of these two models are generally similar. Overall, the ATIL-V model provides a better representation of the lightning return stroke in terms of predicted currents and electromagnetic fields. The proposed model is a step forward to finding a method to reduce the speed of current waves propagating on a vertical conductor in air, such that the evolution of wave shape is consistent with optical observations of lightning.

APPENDIX A

PROPAGATION SPEED FOR A NONUNIFORM TRANSMISSION LINE

In order to illustrate the effect of the difference in speeds of the antenna-mode and TL-mode currents on the observed current dispersion, we consider a two-wire TL with varying angle between the wires, as shown in Fig. 8. The opening angle θ varies from 0° (horizontal wire and its image or parallel wire TL) to 90° (vertical monopole and its image or dipole). The length of each wire is 4.5 km and the separation between the two wires at the source end is 30 m. Current waveforms on one of the wires 2 km from the source for different values of the opening angle are calculated using the same numerical method as in the ATIL-F model. Results for two cases, $L^{\rm add}=0$, $R=0.07\ \Omega$/m and $L^{\rm add}=6.75\times10^{-6}$ H/m, $R=0.4\ \Omega$/m are shown in Fig. 9. As seen in Fig. 9(a), due to equal propagation speeds for both TL-mode and antenna-mode components for the case of $L^{\rm add}=0$, the dispersion for different opening angles is essentially the same. For the inductively loaded parallel wire TL ($\theta=0$), the antenna-mode component is negligible [28], [32], and hence, the amount of dispersion is low [Fig. 9(b)]. On the other hand, for $\theta>2°$ dispersion increases significantly with increasing the opening angle. For the inductively loaded vertical monopole and its image ($\theta=90°$), which is the same configuration as that used in the ATIL model, the antenna-mode current is appreciable and, as a result, considerable dispersion is observed. Although the distributed resistance is different for the two cases under consideration (for reasons discussed in Section IV-B1), simulations show that for $R<0.5\ \Omega$/m, the effect of distributed resistance (compared to distributed inductance) on dispersion and propagation speed is negligible. Detailed discussion of the effect of R on the dispersion and propagation speed is outside the scope of this paper.

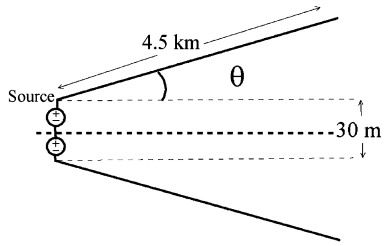

Fig. 8. Two-wire TL with varying opening angle ($0<\theta<90°$), used to illustrate the relation between the current dispersion and different propagation speeds for the antenna and TL current modes. The TL is uniform for $\theta=0$ and nonuniform for $\theta>0$.

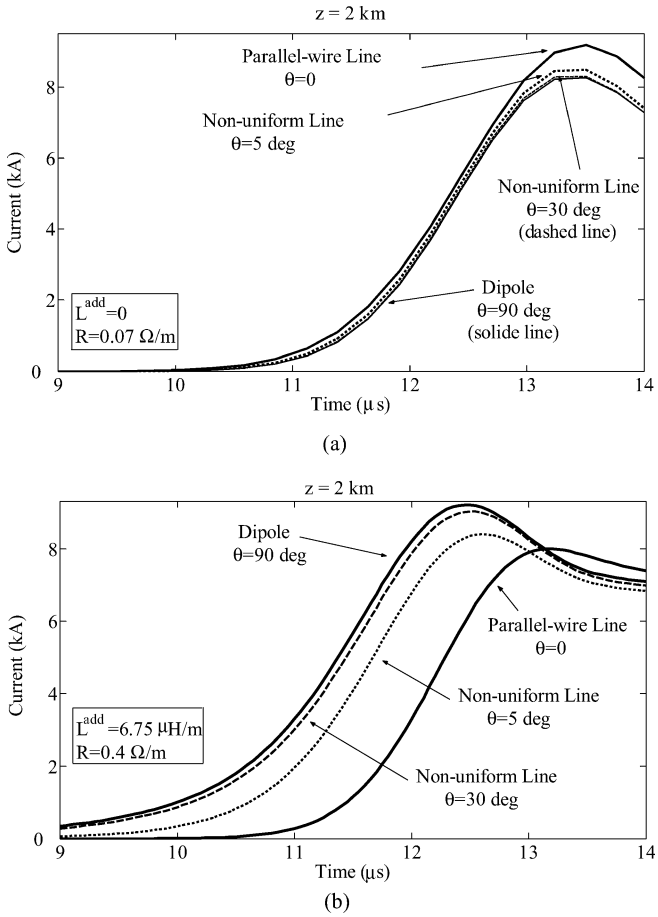

Fig. 9. Effect of opening angle θ on dispersion and propagation speed of current pulses on two-wire TL shown in Fig. 8 for (a) $L^{\rm add}=0$ (no inductive loading), $R=0.07\ \Omega$/m and (b) $L^{\rm add}=6.75\times10^{-6}$ H/m, $R=0.4\ \Omega$/m. Current waveforms are shown for a distance of 2 km from the source.

The aforementioned approach can be used to explain the relatively small dispersion in the AT model. In this model, the propagation speed for the antenna-mode current is equal to 1.3×10^{8} m/s, because the relative permittivity of medium is set to 5.3. The propagation speed for the TL-mode current component is slightly less than 1.3×10^{8} m/s due to the effect of resistive loading. Since the difference between the speeds of these two current components is insignificant, relatively small dispersion is observed.

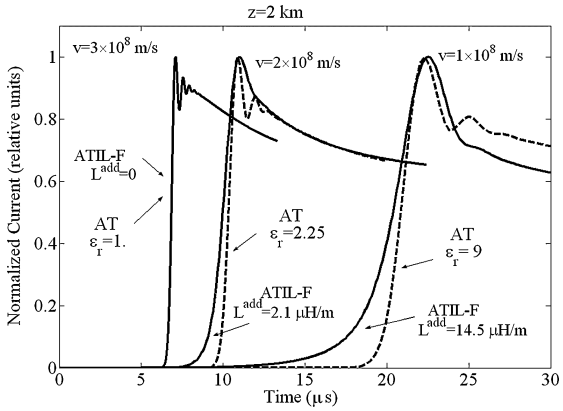

Fig. 10. Illustration of the current dispersion as a function of propagation speed for the AT and ATIL-F models. Current versus time waveforms are computed at $z = 2$ km for three different values of speed, 3×10^8, 2×10^8, and 1×10^8 m/s, which were achieved by adjusting ε_r in the AT model and L^{add} in the ATIL-F model. Resistive loading was 0.07 and 0.4 Ω/m for the AT and ATIL-F models, respectively.

The effect of propagation speed on current dispersion is additionally examined using the speed adjustment methods implemented in the AT (higher permittivity medium) and ATIL-F (inductive loading) models. Fig. 10 shows current in the channel at a distance of 2 km from the channel base. In order to achieve $v = 3 \times 10^8$, 2×10^8, and 1×10^8 m/s in the AT model, we set $\varepsilon_r = 1$, 2.25, and 9, respectively, and in the ATIL-F model, we use $L^{\mathrm{add}} = 0, 2.1 \times 10^{-6}$, and 14.5×10^{-6} H/m, respectively. The AT model predicts relatively small current dispersion for all three propagation speed, while in the ATIL-F model, dispersion decreases appreciably with increasing propagation speed.

ACKNOWLEDGMENT

The authors would like to thank the three anonymous reviewers for their comments.

REFERENCES

[1] C. A. Nucci, G. Diendorfer, M. Uman, F. Rachidi, M. Ianoz, and C. Mazzetti, "Lightning return stroke current models with specified channel base current: A review and comparison," *J. Geophys. Res.*, vol. 95, pp. 20 395–20 408, Nov. 1990.

[2] R. Tottappillil and M. Uman, "Comparison of lightning return stroke models," *J. Geophys. Res.*, vol. 98, no. D12, pp. 22 903–22 914, Dec. 1993.

[3] R. Tottappillil, D. K. McLain, M. A. Uman, and G. Diendorfer, "Extension of Diendorfer–Uman lightning return stroke model to the case of a variable upward return stroke speed and a variable downward discharge current speed," *J. Geophys. Res.*, vol. 96, pp. 17 143–17 150, 1991.

[4] V. A. Rakov and M. A. Uman, "Review and evaluation of lightning return stroke models including some aspects of their applications," *IEEE Trans. Eelectromagn. Compat.*, vol. 40, no. 4, pp. 403–426, Nov. 1998.

[5] B. Kordi, R. Moini, and V. A. Rakov, "Comparison of lightning return stroke electric fields predicted by the transmission line and antenna theory models," in *Proc. 15th Int. Zurich Symp. Electromagn. Compat.*, Zurich, Switzerland, Feb. 2003, pp. 551–556.

[6] V. A. Rakov, "Lightning return stroke speed: A review of experimental data," in *Proc. Int. Conf. Lightning Protection*, Avignon, France, 2004, pp. 139–144.

[7] V. P. Idone and R. E. Orville, "Lightning return stroke velocities in the Thunderstorm Research International Program (TRIP)," *J. Geophys. Res.*, vol. 87, pp. 4903–4915, 1982.

[8] J. E. Borovski, "An electrodynamic description of lightning return strokes and dart leaders: Guided wave propagation along conducting cylindrical channels," *J. Geophys. Res.*, vol. 100, no. D2, pp. 2697–2726, Feb. 1995.

[9] C. E. Baum, "Return-stroke initiation," in *Proc. EMC Symp.*, Zurich, Switzerland, 1989, pp. 383–388.

[10] C. E. Baum and L. Baker, "Analytic return-stroke transmission-line model," in *Lightning Electromagnetics*, R. L. Gardner, Ed. New York: Taylor & Francis, 1990, pp. 17–45.

[11] D. Wang, N. Takagi, T. Watanabe, V. A. Rakov, and M. A. Uman, "Observed leader and return-stroke propagation characteristics in the buttom 400 m of a rocket triggered lightning channel," *J. Geophys. Res.*, vol. 104, no. D12, pp. 14 369–14 376, Jun. 1999.

[12] A. S. Podgorski and J. A. Landt, "Numerical analysis of the lightning CN-tower interaction," presented at the Int. Zurich Symp. Electromagn. Compat., Zurich, Switzerland, 1985.

[13] V. A. Rakov and A. A. Dulzon, "Calculated electromagnetic fields of lightning return strokes," *Tech. Elektrodinamika*, vol. 1, pp. 87–89, 1987.

[14] M. Rubinstein and M. A. Uman, "Transient electric and magnetic fields associated with establishing a finite electrostatic dipole, revisited," *IEEE Trans. Electromagn. Compat.*, vol. 33, no. 4, pp. 312–320, Nov. 1991.

[15] R. Moini, V. A. Rakov, M. A. Uman, and B. Kordi, "An antenna theory model for the lightning return stroke," presented at the Int. Zurich Symp. Electromagn. Compat., Zurich, Switzerland, 1997.

[16] R. Moini, B. Kordi, G. Z. Rafi, and V. A. Rakov, "A new lightning return stroke model based on antenna theory model," *J. Geophys. Res.*, vol. 105, no. D24, pp. 29 693–29 702, Dec. 2000.

[17] R. Moini, B. Kordi, and M. Abedi, "Evaluation of LEMP effect on complex wire structure located above a perfectly conducting ground using electric field integral equation in time domain," *IEEE Trans. Electromagn. Compat.*, vol. 40, no. 2, pp. 154–162, May 1998.

[18] B. Kordi, R. Moini, and H. Alaghemand, "Evaluation of the lightning induced over-voltages in sagged transmission lines using electric field integral equation in time domain," presented at the Proc. Int. Conf. Lightning Protection, Birmingham, U.K., 1998.

[19] F. Bost, L. Nikolas, and G. Rojat, "Study of conduction and induction phenomena in electric circuits using a time-domain Integral formulation," *IEEE Trans. Magn.*, vol. 36, no. 4, pp. 960–963, Jul. 2000.

[20] M. R. Guedira, "Etude en regime transitoire du comportement de structures filaires presentant de charges lineraires ou non lineraires," Ph.D. thesis. Limoges, France: Univ. Limoges, 1983.

[21] C. A. Nucci, S. Guerrieri, M. T. Correia de Barros, and F. Rachidi, "Influence of corona on the voltages induced by nearby lightning on overhead distribution lines," *IEEE Trans. Power Del.*, vol. 15, no. 4, pp. 1265–1273, Oct. 2000.

[22] S. Bonyadi-Ram, R. Moini, S. H. H. Sadeghi, and V. A. Rakov, "Incorporation of distributed capacitive loads in the antenna theory model of lightning return stroke channel," in *Proc. 25th Int. Zurich Symp. Electromagn. Compat.*, 2005, pp. 213–218.

[23] S. Bonyadi-Ram, R. Moini, and S. H. H. Sadeghi, "Incorporation of distributed inductive loads in the antenna theory model of lightning return stroke channel," in *Proc. Int. Conf. Lightning Protection*, Avignon, France, 2004, pp. 101–105.

[24] Y. Baba and M. Ishii, "Characteristics of electromagnetic return-stroke models," *IEEE Trans. Electromagn. Compat.*, vol. 45, no. 1, pp. 129–135, Feb. 2003.

[25] E. K. Miller, "An integro-differential technique for time-domain analysis of thin wire structures," *J. Comput. Phys.*, vol. 12, pp. 24–48, 1973.

[26] R. C. Olsen, III, D. M. Jordan, V. A. Rakov, M. A. Uman, and N. Grimes, "Observed one-dimensional return stroke propagation speeds in the bottom 170 m of a rocket triggered lightning channel," *Geophys. Res. Lett.*, vol. 31, no. 16, pp. L16107-1–L16107-4, 2004.

[27] E. M. Bazelyan, B. N. Gorin, and V. I. Levitov, *Physical and Engineering Foundations of Lightning Protection*. St. Petersburg, Russia: Gidrometeoizdat, 1978.

[28] V. Kodali, V. A. Rakov, M. A. Uman, K. J. Rambo, G. H. Schentzer, J. Schoene, and J. Jerauld, "Triggered-lightning properties inferred from measured currents and very close electric fields," *Atmos. Res.*, vol. 76, pp. 355–376, 2005.

[29] D. M. Jordan and M. A. Uman, "Variation in light intensity with height and time from subsequent lightning return stroke," *J. Geophys. Res.*, vol. 88, pp. 6555–6562, 1983.

[30] C. R. Paul, *Analysis of Multi-Conductor Transmission Lines*. New York: Wiley, 1994.

[31] Y. M. Lin, M. A. Uman, J. A. Tiller, R. D. Brantley, W. H. Beasley, E. P. Krider, and C. D. Weidman, "Characterization of lightning return stroke electric and magnetic fields from simulations two-station measurements," *J. Geophys. Res.*, vol. 84, pp. 6307–6314, 1979.
[32] M. N. Sadiku, *Numerical Techniques in Electromagnetics*. Boca Raton, FL: CRC, 1992.
[33] Y. Baba and V. A. Rakov, "On the mechanism of attenuation of current waves propagating along a vertical perfectly conducting wire above ground: application to lightning," *IEEE Trans. Electromagn. Compat.*, vol. 47, no. 3, pp. 521–532, Aug. 2005.

Siamak Bonyadi-Ram received the B.S. degree in electrical (telecommunications) engineering from the Sharif University of Technology, Tehran, Iran, in 1994, and the M.S. and Ph.D. degree in electrical engineering from the Amirkabir University of Technology (Tehran Polytechnic), Tehran, in 1997 and 2005, respectively.

From 1998 to 2006, he was with the Communication Regulatory Authority of Iran as a Radio Frequency Spectrum Expert. He is currently a Postdoctoral Fellow at the University of Manitoba, Winnipeg, MB, Canada. He is also with the Electromagnetics Research Laboratory, Amirkabir University of Technology, Tehran. His current research interests include radio wave propagation, electromagnetic compatibility measurements and modeling (especially in lightning), and time-domain numerical solution of electromagnetics problems.

Rouzbeh Moini (A'89–M'93–SM'06) was born in Tehran, Iran, in 1963. He received the B.S., M.S., and Ph.D. degrees in electronics from Limoges University, Limoges, France.

In 1988, he joined the Electrical Engineering Department, Amirkabir University, Tehran, where he is currently a Professor of telecommunications. During 1995–1996, he was a Visiting Professor at the University of Florida, Gainesville. His current research interests include numerical methods in electromagnetics, electromagnetic compatibility, and antenna theory.

Dr. Moini is the recipient of the 1995 Islamic Development Bank Merit Scholarship Award.

S. H. H. Sadeghi (M'92–SM'05) received the B.S. degree in electrical engineering from the Sharif University of Technology, Tehran, Iran, the M.S. degree in power engineering from the University of Manchester Institute of Science and Technology, Manchester, U.K., and the Ph.D. degree in electronic systems engineering from the University of Essex, Colchester, U.K., in 1980, 1984, and 1991, respectively.

During 1980–1983, he was with the Electrical Power Industry, Tehran. During 1984, he was a Research Assistant at the University of Lancaster, Lancaster, U.K. He was with the University of Essex as a Senior Research Officer. In 1992, he was appointed as a Research Assistant Professor at Vanderbilt University, Nashville, TN. During 1996–1997, and 2005–2006 he was a Visiting Professor at the University of Wisconsin, Milwaukee. He is currently a Professor of electrical engineering at the Amirkabir University of Technology, Tehran. His current research interests include electromagnetic nondestructive testing of materials and electromagnetic compatibility problems in power engineering.

Vladimir A. Rakov (SM'96–F'03) received the Master's and Ph.D. degrees from Tomsk Polytechnical University (Tomsk Polytechnic), Tomsk, Russia, in 1977 and 1983, respectively, all in electrical engineering.

From 1977 to 1979, he was an Assistant Professor of electrical engineering at Tomsk Polytechnic. In 1978, he was involved in lightning research at the High Voltage Research Institute, a division of Tomsk Polytechnic, where from 1984 to 1994, he was the Director of the Lightning Research Laboratory. He is currently a Professor in the Department of Electrical and Computer Engineering, University of Florida, Gainesville. He is the author or coauthor of over 30 patents, one book, and over 300 papers and technical reports on various aspects of lightning.

Dr. Rakov is the Chairman of the Technical Committee on Lightning of the Biennial International Zurich Symposium on Electromagnetic Compatibility and a former Chairman of the American Geophysical Union Committee on Atmospheric and Space Electricity. He is a Fellow of the American Meteorological Society.